

Multispectral Processing Methods to Recover Text from the World Map by Martellus (c. 1491)

ROGER L. EASTON, JR., Chester F. Carlson Center for Imaging Science, Rochester Institute of Technology, Rochester NY, USA

CHET VAN DUZER, David Rumsey Fellow, John Carter Brown Library, Providence RI, USA

KEVIN SACCA, Blue Origin, Seattle WA, USA

The c. 1491 world map by Henricus Martellus Germanus, in the collection of the Beinecke Rare Book and Manuscript Library of Yale University, is a very important visual and historical object, being very similar to the c. 1492 globe by Martin Behaim and evidently having influenced the 1507 world map by Martin Waldseemüller to a significant degree. Martellus' map is painted on paper sheets mounted on canvas and most of the area is covered with text, nearly all of which has faded to the point where it is not readable to the unaided eye. Because of this condition, the map had been little studied, even though it had the promise of yielding significant insight about the geographical knowledge of the time.

The Martellus map was imaged by a team of scientists and scholars in August 2014. Though significant information was recovered during the imaging session, the subsequent spectral image processing required more than a year. Because of the different colors used for both texts and backgrounds (to represent different types of physical features), customized processing methods were necessary to recover many of the writings. From the results, it is estimated that more than 80 % of the writings have now been recovered, vs. less than 10 % available to the eye from the original map.

This paper will review the spectral image processing methods used to recover the texts, including discussions of necessary preprocessing methods to balance the contrast of the text and background, useful segmentation algorithms, as well as post processing methods used to enhance the text visibility further.

Key words:

Martellus World Map, multispectral imaging, spectral image processing, principal component analysis, independent component analysis, minimum noise fraction transform.

CHNT Reference:

Roger L. Easton, Jr. et al. Processing Methods to Recover Text Information from Multispectral Imagery of the World Map by Henricus Martellus (c. 1491).

INTRODUCTION

The large world map (c. 2 m × 1.22 m), made by Henricus Martellus about the year 1491, is widely acknowledged to be of great importance in the history of cartography. The map likely was the best contemporary cartographic representation of the geographical concepts of the earth when Christopher Columbus made his first voyage, and there are good reasons for the belief that Columbus saw this map or another similar one by Martellus, and that the map influenced Columbus's ideas about the world's geography.

Because of the fading of its descriptive texts and place names, the map had been little studied since it first came to the attention of scholars in 1959. An effort to image the map was supported by funding from the USA National Endowment for the Humanities in 2014. The team visited the Beinecke Rare Book and Manuscript Library at Yale

□

Authors addresses: Roger L. Easton, Jr., Chester F. Carlson Center for Imaging Science, Rochester Institute of Technology, Rochester NY, USA 14623-5605; email: easton@cis.rit.edu; Chet Van Duzer, David Rumsey Research Fellow, John Carter Brown Library, Brown University, Providence RI, USA, 02906; email: chet.van.duzer@gmail.com; Kevin Sacca, Blue Origin, Kent, WA, USA 98032; email: kwsacca@gmail.com.

University to collect imagery of the map for subsequent image processing with the goal of recovering the texts on the map and making it available to scholarship. The map proved to be an excellent candidate for spectral imaging, and this paper describes the imaging processing methods applied to the data and the results obtained. The visual appearance of the map is shown in Fig. 1.



Fig. 1. Visual appearance of the c. 1491 world map by Henricus Martellus Germanus. The various texts are not visible at this scale, but processing reveals that the landforms are covered with texts. Text on the water surfaces is placed only on the islands and cartouches

IMAGE COLLECTION

Because of their relevance to the subsequent image processing, it will be useful to consider the illumination and camera system used for multispectral image collection, which is very similar to that currently used at a number of institutions, including the British Library, the Centre for the Study of Manuscript Cultures at the University of Hamburg, and St. Catherine's Monastery [Easton et al. 2010]. The map was illuminated by light from panels of light emitting diodes (LEDs) in 12 bands from the near-ultraviolet band centered at 365 nm, five bands in the visible range (centered at 450 nm, 470 nm, 505 nm, 535 nm, 570 nm, 635 nm), and five bands in the infrared region (centered at 700 nm, 735 nm, 780 nm, 870 nm, 940 nm). In addition, (and important for subsequent processing), spectral images of induced fluorescence were collected by illuminating the map with light at 365 nm and 455 nm and imaging through four Wratten gelatin filters, which transmitted blue, green, orange, and red light. The blue filter #47 transmits light in the range $410 \text{ nm} \lesssim \lambda \lesssim 500 \text{ nm}$, the green filter #58 transmits $500 \text{ nm} \lesssim \lambda \lesssim 580 \text{ nm}$, orange #22 passes wavelengths longer than 560 nm, and #25 passes wavelengths longer than 590 nm. In addition, images generated by ultraviolet illumination were collected through "ultraviolet passing" and "ultraviolet blocking" filters. Images using the former modality produce an image of the reflected ultraviolet light, while the latter images the integrated fluorescence. A total of 22 spectra bands were collected for each map tile: 12 in reflection, six in fluorescence under ultraviolet illumination, and four in fluorescence under blue illumination.

Note that images are collected over at wavelengths in the range $365 \text{ nm} \lesssim \lambda \lesssim 940 \text{ nm}$, which is nearly twice the bandwidth of visible light ($400 \text{ nm} \lesssim \lambda \lesssim 700 \text{ nm}$). For this reason, it was important to use a "spectral" lens that is designed for this purpose rather than using an "off-the-shelf" normal lens designed for imaging only in the visible

range would be noticeably defocused for light near the extrema of the wavelengths of illumination. A macro lens with focal length $f = 120$ mm and focal ratio $f/4.5$ was designed and fabricated to specification by Brian Caldwell of *Caldwell Photographic*. This lens allows collection of images over the full range at the same focus setting and with resolution near the diffraction limit.

Imagery was collected using the E7 camera from Megavision, Inc., which includes the KAF-50100 50-megapixel sensor, with 8176×6132 pixels of size $6 \mu\text{m}$ square, resulting in a sensor with dimensions $49.1 \text{ mm} \times 36.8 \text{ mm}$. The larger pixels in this sensor results in improved noise statistics when compared to newer sensors with smaller pixels. This compromise between pixel count and noise response is very important when imaging faint sources, as in the case of fluorescence generated by ultraviolet stimulation but observed in red light. The images have 13 bits of measured dynamic range.

Due to its large size, the map was imaged in 55 “tiles” (11 horizontally by five vertically) with the sensor oriented in “portrait” format (long dimension vertical), with 15 % overlap for subsequent stitching of collected images. Each tile covered an area of approximately $280 \text{ mm} \times 210 \text{ mm}$ at a resolution of approximately 29.2 pixels per mm (~ 735 pixels per inch).

The map was supported on a large easel that allowed the map to be translated horizontally and vertically to position individual tiles in front of the lights and camera in the same geometry. To ensure the same plate scale for each tile, vertical lines of light from solid-state lasers were projected at tilts so that the lines converged to form a single line when the map was positioned at the proper distance from the camera. The camera and laser line projectors were mounted on a “StackShot” focusing rail that allowed precise movement of both towards or away from the map. By adjusting the distance of the camera using the StackShot until the lines of laser light merged, it was possible to ensure accurate focus for each tile easily and quickly. The time required to collect a full set of images for one tile was approximately four minutes.

Because statistical image processing was planned, accurate calibration of the spectral imagery was important. The reflectance was calibrated from images of reference targets composed of both broadband reflectance standards made of Spectralon[®] by Labsphere, Inc. (with three broadband reflectances of 2 %, 50 %, and 99 % over the range $250 \text{ nm} \lesssim \lambda \lesssim 2500 \text{ nm}$) and a ColorChecker chart from X Rite Photo. It is important to note that the reflectances of the X Rite chart are calibrated only for visible light and are not well suited to use outside of this range. Since it was not possible to include the standard objects in each tile, the standards were imaged at the beginning and conclusion of each collection and the statistics transferred to images of the individual tiles.

The image data were saved as “raw” digital negative files and as “flattened” files evaluated from the ratio of the raw data and the flat-field images. The metadata from the image collection are recorded during image capture and inserted in the header of the raw and flattened image files.

A snapshot showing the map on the imaging easel and the camera is presented in Fig. 2.



Fig. 2. Martellus map mounted on moveable easel with Megavision E7 camera

The wavelengths, f /stops, and exposure times for each band are listed in Fig. 3. All reflection bands were imaged at $f/12.5$. Note the larger apertures and longer exposure times for the fluorescence bands, which were necessary to reduce the ultraviolet exposure to the map. Despite these longer exposures, the fluorescence bands often exhibited significant variations due to the statistical uncertainties. The statistical “salt-and-pepper” noise was generally reduced by applying at 3×3 median filter to these fluorescence bands before subsequent processing.

Reflection			Fluorescence				
Center λ	f /#	Exp time (s)	Illumination	Filter	f /#	Exp. Time (s)	
365nm	$f/12.5$	5.244 s	365nm	B47	$f/5.6$	20.000 s	
450nm	$f/12.5$	0.613 s		G58	$f/5.6$	20.000 s	
470nm	$f/12.5$	0.542 s		O22	$f/5.6$	20.000 s	
505nm	$f/12.5$	0.800 s		R25	$f/5.6$	20.000 s	
535nm	$f/12.5$	0.874 s		UV block	$f/5.6$	5.000 s	
580nm	$f/12.5$	0.893 s		UV pass	$f/5.6$	20.000 s	
625nm	$f/12.5$	0.500 s		450nm	B47	$f/5.6$	0.500 s
700nm	$f/12.5$	11.648 s			G58	$f/5.6$	5.000 s
735nm	$f/12.5$	5.100 s			O22	$f/5.6$	5.000 s
780nm	$f/12.5$	3.809 s			R25	$f/5.6$	10.000 s
870nm	$f/12.5$	3.449 s					
940nm	$f/12.5$	11.784 s					

$\Delta\lambda \approx 40\text{nm}$

Fig. 3. The wavelengths, f /stop settings, bandpass filter, and exposure times for the 22 collected bands

IMAGE PROCESSING

The goal of the image processing is to select combinations of the collected spectral bands that enhance the visibility of the faded writings. This objective is closely related to that of recovering erased text from erased and overwritten (“palimpsested”) parchment manuscripts, which fortunately is a familiar task for the imaging team, having worked on the Archimedes palimpsest [Christens-Barry et al. 2011], the Syriac-Galen medical palimpsest [Easton et al. 2018], the “New Finds” palimpsests from St. Catherine’s Monastery, and the “Dexippus” palimpsest in Vienna, among others.

In palimpsest imaging, the goal is enhancement and/or segmentation of two (occasionally of three) texts that usually were written in iron gall ink. The erased writings often could be made readable by “deterministic” methods, which could be as simple as choosing the best band for reading the text from the set of collected images or by rendering two or three selected bands in pseudocolor. In the case of the Martellus map, where text is written in several colors of pigment laid over different background colors, and is therefore significantly more complex than processing of most palimpsest imagery.

Because of the different background pigments in the scene, particularly near coastlines, it was useful to “preprocess” the spectral imagery to normalize the contrast. This was accomplished by a method we have dubbed “blur and divide,” but which was called “pseudo-unsharp masking” during an effort to enhance details in images of solar corona and comet tails, where the wide variation in background often obscures the fine details of interest [Matuska et al. 1978]. The name was applied based on the resemblance to the well-known photographic method of “unsharp masking,” where a blurred negative is combined with the original positive to a difference “sharpened” image. Because the “blur-and-divide” operation removes much of the wide variation in the image statistics, the results of the subsequent image processing tools often exhibit improvements.

The ENVI[®] software package from Harris Corporation was used for most of the spectral image processing of the Martellus map. ENVI[®] is commonly used to process environmental spectral imagery collected from aircraft and spacecraft, but is very appropriate for this “near-field” remote sensing task. It includes a wide range of imaging software tools, including some for common image processing (such as contrast enhancement and registration/stitching), but its primary value in this project is due to the efficient software for statistical image

segmentation. ENVI[®] operates on spatial-spectral image “cubes” (three-dimensional data arrays) created from the images, followed by gray-scale calibration based on the images captured of the Spectralon[®] and X Rite reflectance standards.

The first steps in the task workflow are the “preprocessing” (creation of the image cubes, calibration based on the reflectance standards, and pseudo-unsharp “blur and divide”). The bands are examined for noticeable features and to select local areas where the statistics are evaluated that are to be used in the subsequent transformations. Because the final image results depend on the statistics, this adds another level to the iterative nature of the workflow. The bands are processed using methods to be described, and the resulting output images were rendered in RGB “pseudocolor,” and subsequently enhanced in Adobe Photoshop[®] to rotate the hue angle of the pseudocolor rendering and/or to enhance the contrast. The images selected from the processing were delivered to one of the authors (CVD), who assessed the result and delivered feedback and identified regions for the subsequent iteration.

The first processing method applied usually was the well-known Principal Component Analysis (PCA), but the Minimum Noise Fraction Transform (MNF), and Independent Component Analysis (ICA) were also used with good results. Because of the different combinations of pigments used for text and background and the different conditions in different locations on the map, a wide variety of processing methods were applied to the same tile. Often, the results of one process showed the locations of previously unseen text, which led to subsequent processing for that region. The processing proceeded iteratively and the best results from these were subsequently combined to produce output images of readable text.

PCA was originally suggested by Pearson [1901]. The process combines N images in a set of spectral bands to create a new set of N uncorrelated bands using only second-order statistics. In other words, the data are assumed to be Gaussian distributed. The two sets are “equivalent” because both “forward” and “inverse” transformations are specified, which allows the original band set to be reconstructed from the PCA bands. Because the new bands are “uncorrelated,” any statistical similarities among the images in the original set of bands will not exist in the set resulting from the processing. The bands in the PCA set are sequenced by statistical “variance;” the band with the largest variance (and therefore the widest range in numerical values) appears first in the sequence, while each succeeding processed band exhibits less variance than the previous output band in the sequence. In this way, the highest-order calculated bands exhibit the smallest variance and therefore the smallest variation in image contrast. Often these highest-order bands include any random “noise” variations in the image data, while the lowest-order bands include the “true” image structure. Since the noise is now segregated from bands with “nonrandom” (i.e., “real”) variations in structure, the noise may be discarded and the PCA calculation inverted to reconstruct the original image bands without the random noise. By this method, PCA becomes useful for “denoising” the image data. It also is a method for evaluating the effective number of image bands in the original data.

MNF [Green et al. 1988] also transforms the set of N image bands into a new set of N bands that are sequenced according to a noise-content description of “image quality.” It has been used effectively for “denoising” of hyperspectral image data. Its end result is similar to that from PCA, but MNF often does a better and more reliable job of identifying and removing noise from the data than is possible with PCA alone. The goal of MNF is to identify component bands that are more important to the signal-to-noise ratio (SNR) of the ensemble of bands.

The goal of ICA [Hyvarinen 1999] is to separate the N spectral input bands into individual “signals” generated by individual constituent components. In this sense, ICA resembles PCA, but the output bands are statistically “independent” rather than statistically “uncorrelated.” Since the former criterion is stronger than that in PCA, the assumptions made about the image data in ICA are less stringent and higher-order statistical correlations are used. A common illustration of ICA is to solve the so-called “cocktail party problem,” where a listener hears a mixture of sounds from several independent conversations, but needs to isolate the individual chats. The collected dataset comprises recordings from different microphones scattered about the room, where each records a combination of sounds from all conversations. An individual recorded signal from the microphones is analogous to the set of spectral image bands and the individual conversations are analogous to individual features on the map. The ICA calculation looks for differences in the measured signals that satisfy the condition for statistical independence. If the different conversations are truly independent (as they would usually be in a cocktail party), ICA usually is able to segment the signals into their constituent components. In the map problem, the statistical independence of the individual signals is less certain due to the overlap of the pigment spectra.

Not surprisingly, the output bands obtained from the different algorithms exhibited variations in the visibility of the text with location. For this reason, individual bands from the different methods often were combined to form pseudocolor images. These were exported to “general-purpose” image processing tools, such as Adobe Photoshop[®]

for subsequent enhancement of contrast and to rotate the hue angle with the goal of maximizing the visibility of the texts of interest.

RESULTS

Though it might be desirable to illustrate the value of the different image processing methods for the entire map, the limitations of space make it necessary to select a small number of examples. One specific region on the map was selected for illustration, where texts were written in at least two different pigments. The location is the coast of southwest Africa, where the brownish pigment used for the landmass evidently is “thicker” at the boundary with the blue pigment used for the Atlantic Ocean. This additional thickness can obscure the writings for the names of rivers and villages near the coast. One example for the tile C03R04 (third column, fourth row) is shown in Fig. 4. Very little, if any, text is visible to the eye (Fig. 4a), but significant text is readable in Fig. 4b, which is a pseudocolor image evaluated from all 22 bands and displayed with PC bands 2, 8 and 22 in the red, green, and blue channels, respectively. The additional pigment thickness produces a “murky” area near the coast that can obscure some characters. In these conditions, evaluating the ratio of each band and its replica blurred over a scale larger than the text characters (a 201×201 window was used in this case), can reveal additional writings, as shown in Fig. 4c, which is a pseudocolor constructed from the ICA transformation of the original set of 22 bands. .

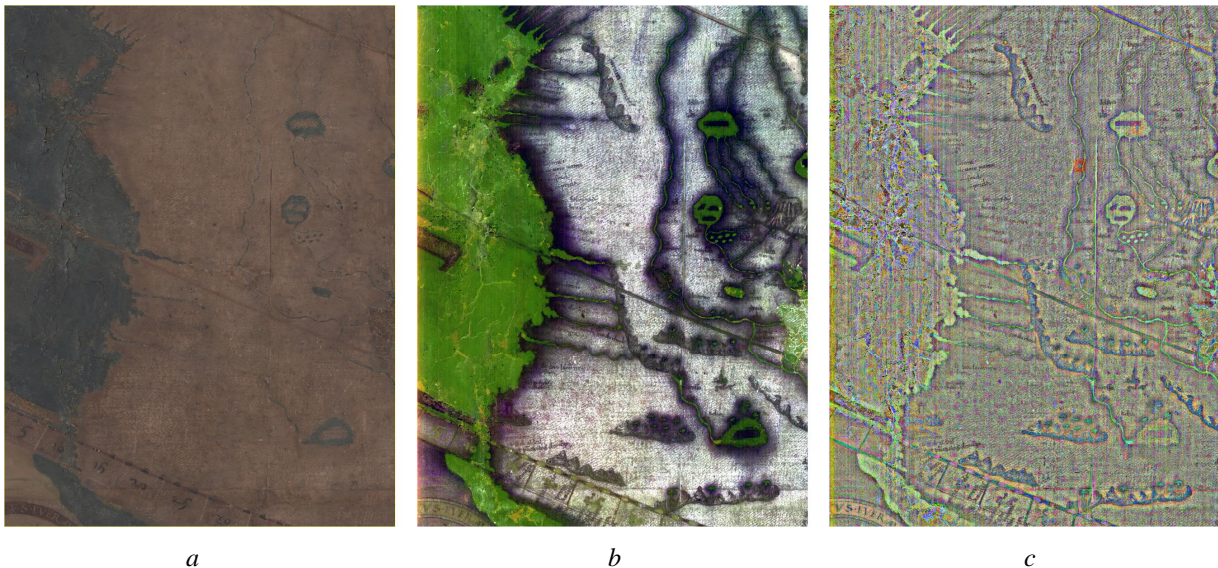


Fig. 4. Tile C03R04 of the Martellus map showing the coast of southwestern Africa a) visual appearance, showing very little text, b) pseudocolor image from PCA bands (PC band 2 in red, band 8 in green, band 22 in blue), and c) pseudocolor image from three ICA bands after implementing “blur and divide” over a region of 201 pixels square (IC band 17 in red, band 18 in green, band 20 in blue)

However, some text is still not visible in these output images, even with the “blur and divide.” For example, consider the results in Fig. 5, which shows a magnified section of the same tile C03R04. Some text is clearly visible in the first example, which is the ratio of two image bands (red fluorescence under blue illumination divided by the infrared band centered at 940nm), but gaps between the writings over the river courses suggests that additional text might exist. The recovery of this text was difficult, suggesting that the particular pigment for that writing has faded more than the other pigments. Some characters were recovered by combining PCA and ICA processing of subsets of the original image bands. A result is shown in Fig. 5.

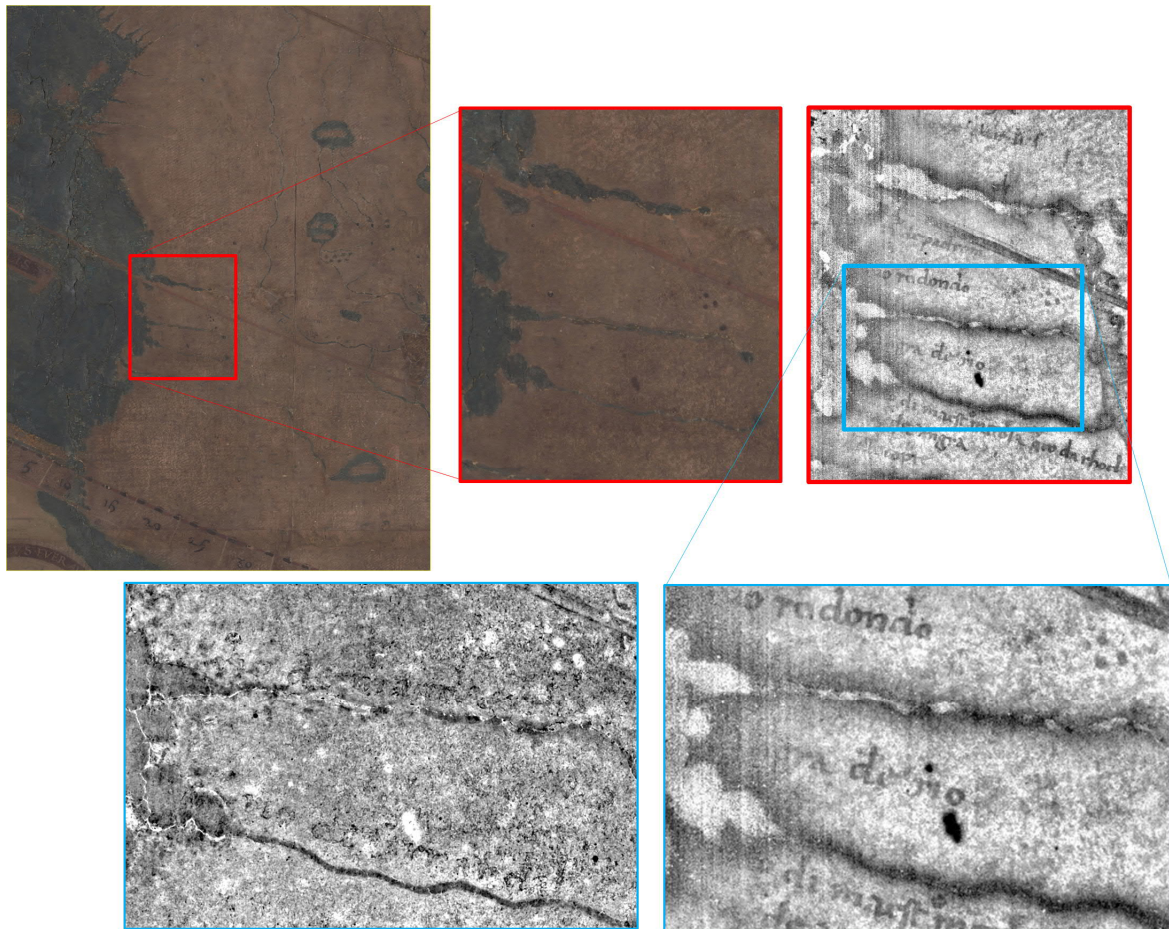


Fig. 5. Processing to recover river names from tile C03R04 of the Martellus map. The visual appearance of the magnified section is compared to processing results after “blur and divide” of PCA on 6 selected bands (bottom left) and infrared band ratios (bottom right), showing that different text is enhanced by the different processing. The PCA revealed names of rivers not available in the band ratio image

CONCLUSIONS

Significant text was recovered from the Martellus map by image processing applied to multispectral image data. The results have led to significant new understanding of the map in the history of cartography. The readings obtained from the imaging have been published [Van Duzer 2018]. This paper offers a more complete description of the methods used.

ACKNOWLEDGEMENTS

The authors thank Nicole Polglaze of Grinnell College (2017 participant in the NSF “Research Experiences for Undergraduates”), Rolando Raqueño (research staff) and Anna Starynska (Ph.D. candidate) of the Chester F. Carlson Center for Imaging Science of RIT, Michael Phelps and Keith Knox of the Early Manuscripts Electronic Library, Kenneth Boydston of Megavision, LLC., and Gregory Heyworth of the University of Rochester, for their very important contributions to this work.

REFERENCES

- William A. Christens-Barry, Roger L. Easton, Jr., and Keith T. Knox. 2011. Imaging and Image Processing Techniques. In Reviel Netz, William Noel, Natalie Tchernetska, and Nigel Wilson, ed. *The Archimedes Palimpsest, Vol. I, Catalogue and Commentary*. Cambridge, 175-207.
- Roger L. Easton, Jr., Keith T. Knox, W.A. Christens-Barry, K. Boydston, M.B. Toth, D. Emery, and W. Noel. 2010. Standardized system for multispectral imaging of palimpsests. In *Proc. of SPIE – Computer Vision and Image Analysis of Art*. Bellingham, WA 98227-0010 -- USA: SPIE vol. 7531-12.
- Roger L. Easton, Jr., Keith T. Knox, William A. Christens-Barry, and Kenneth Boydston. 2018. Spectral imaging methods applied to the Syriac-Galen Palimpsest. *Manuscript Studies* 3, 69-82.
- A.A. Green, M. Berman, P. Switzer, and M.D. Craig. 1988. A transformation for ordering multispectral data in terms of image quality with implications for noise removal: *IEEE Transactions on Geoscience and Remote Sensing*, v. 26, no. 1, p. 65-74.
- A. Hyvarinen. 1999. Fast and robust fixed-point algorithms for independent component analysis, *IEEE Trans. Neural Networks*, vol. 10, no. 3, pp. 626-634.
- Walter Matuska, D.H. Janney, J.A. Farrell, and C.F. Keller, Jr. 1978. Enhancement of Solar Corona and Comet Details, *Optical Engineering* 17(8), 661-665.
- Karl Pearson. 1901. "On Lines and Planes of Closest Fit to Systems of Points in Space," *Philosophical Magazine*. 2 (11): 559–572.
- Chet Van Duzer. 2018. *Henricus Martellus's World Map at Yale (c. 1491)*, Cham, Springer.

Imprint:

Proceedings of the 23rd International Conference on Cultural Heritage and New Technologies 2018. CHNT 23, 2018 (Vienna 2019). <http://www.chnt.at/proceedings-chnt-23/> ISBN 978-3-200-06576-5

Editor/Publisher: Museen der Stadt Wien – Stadtarchäologie

Editorial Team: Wolfgang Börner, Susanne Uhlirz

The editor's office is not responsible for the linguistic correctness of the manuscripts.

Authors are responsible for the contents and copyrights of the illustrations/photographs.